Adjusting PSA amplitudes to V_{S30} = 3000 m / s

David M. Boore

The basic idea, which has been suggested by several authors, is 1) to adjust observed GMIMs (ground-motion intensity measures, including PGV and PGA) to a reference condition (usually $V_{S30} = 760$ m/s) using the site function that appears in GMPEs (usually $\ln GMIM \approx c \ln\left(V_{S30}/V_{REF}\right)$; I anticipate that the coefficient c will come from studies such as those of Hollenback (2014), regressing data in the NGA-East flatfile, or from updated studies such as described by Stewart, 2012, in which amplifications from the PEER NGA-W2 GMPEs are adjusted based on residuals of the NGA-East data relative to the NGA-W2 GMPEs, and 2) then use ratios of simulated PSA computed with stochastic–method simulations which use crustal amplifications for Fourier spectra obtained from models for which $V_{S30} = 760$ m/s and $V_{S30} = 3000$ m/s . In this note I discuss the crustal amplifications for the two values of V_{S30} and then the ratios of GMIMs needed for step 2 (adjusting the GMIM values from sites with $V_{S30} = 760$ m/s to those with $V_{S30} = 3000$ m/s). Included in the section on the crustal amplifications is a discussion of the velocity profiles used for the amplifications. In addition to the ratios of GMIMs for $V_{S30} = 3000$ m/s divided by GMIMs for $V_{S30} = 760$ m/s , I also show GMIM ratios for $V_{S30} = 3000$ m/s divided by the GMIM for $V_{S30} = 2000$ m/s , because many of stations in the NGA-East flatfile have been assigned $V_{S30} = 2000$ m/s (as an aside, I would think that this argues for the reference velocity for NGA-East being 2000 m/s, not 3000 m/s).

The Method

The method is straightforward:

1. Choose a generic velocity profile for the V_{S30} (760, 2000, and 3000 m/s in these notes).

2. Compute crustal amplifications, without attenuation, using the square-root-impedance method (see Boore, 2013).

3. Simulate GMIMs using the stochastic method, as implemented in SMSIM (Boore, 2005) for the three crustal amplifications and several choices of kappa (for the $V_{S30} = 760$ m/s model), for a wide range of **M**, *R*, and *T*.

4. Compute and plot the ratios.

5. Ideally, equations would be fit to the ratios so that the adjustment factor could be easily computed. As will be seen, the ratios are sometimes a strange function of the explanatory variables, and I have not taken the time to find a function that provides a good fit to the ratios. It should be noted that for the magnitudes and distances of most engineering interest that the ratios are often either constant or have a simple variation with the explanatory variables. But this does not help if the need arises to adjust recordings for less important M and R (e.g., **M**=2.5 events) to the reference rock condition. In this case, a lookup of the tables of ratios can be used.

Here is more detail about the steps:

Crustal Amplifications

Sites with $V_{S30} = 760$ m / s

Velocity Profiles for Sites with $V_{S30} = 760$ m/s:

I was provided 6 profiles for which Vs30=760 m/s. three from Walt Silva and three from Hashash and Harmon (HH). As an aside, I think the HH models are unrealistic in that I doubt that velocities of 3 km/s come to with 100 m or so of the surface, but I could be wrong. In addition, I used velocity models from three sites for which Vs30 was close to 760 m/s (HAIL, Vs30=765 m/s, from Odum et al., 2010; HATCH, Baxley, Georgia, Georgia Power Co., Vs30=762 m/s, from J.C. Chin, personal commun.; and OTT, Vs30=755 m/s, from Beresnev and Atkinson, 1997), as well as the BC site condition model from Frankel et al. (1996 [Fea96]; this model was derived by me, in collaboration with Art Frankel—the model replaces a western US model that I used in 1986 with a linear gradient in the upper 200 m with a slope such that Vs30=760 m/s). Because the simulations need velocity profiles extending to depths of at least 8 km, I had to merge the shallow profiles with deeper profiles. I did this by plotting the nine models (three Silva, three HH, HAIL, HATCH, and OTT) along with three shear-wave profiles extending to a depth of 8 km that I had available. These profiles are the one from Fea96, and the Boore and Joyner (1997) (BJ97) generic rock and very hard rock profiles. These profiles are shown in Figure 1.

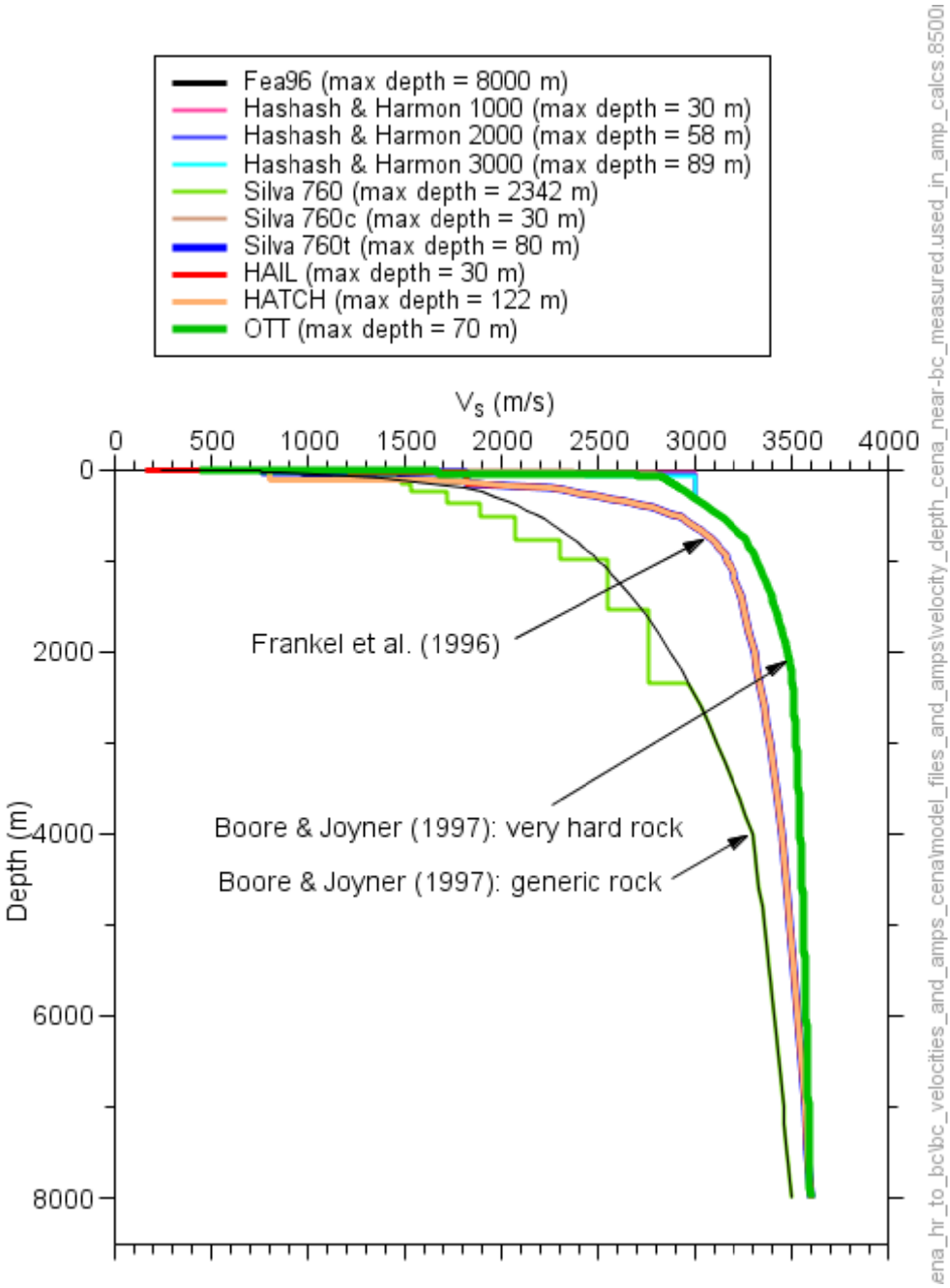

Figure 1. Combined profiles, max depth = 8500 m. The main purpose of this figure is to show the three profiles on to which the shallow profiles were merged.

I then decided on how to extend each model to depth by merging the shallow profile with the deeper profile that seemed most similar to the shallow profile at the deepest part of the shallow profile. The combined profiles are shown for various maximum depths in Figures 1 through 5. In these figures I have not distinguished between the original shallow models and the extended models, but the legends include the maximum depths of each shallow model.

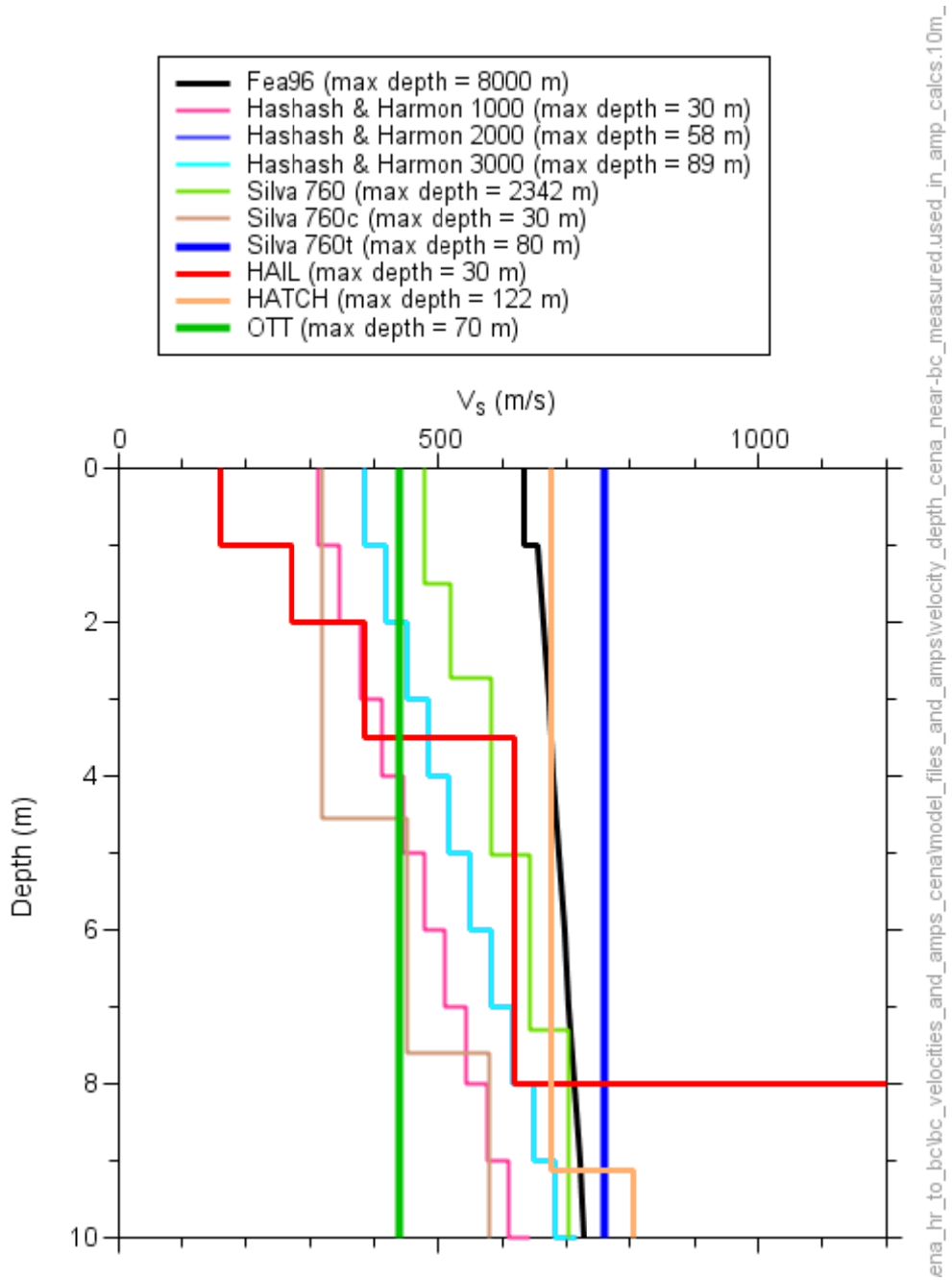

Figure 2. Combined profiles, max depth = 10 m.

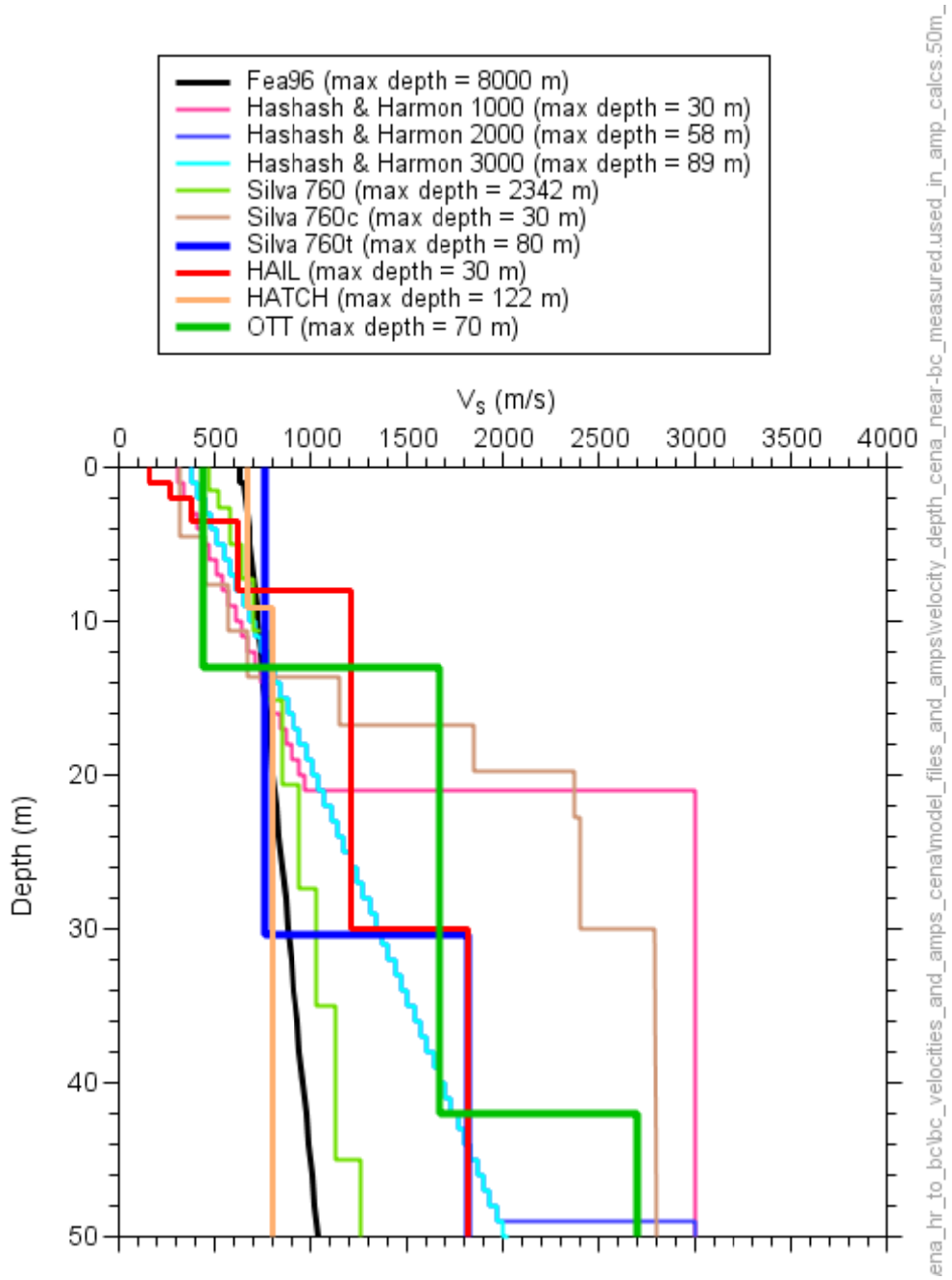

Figure 3. Combined profiles, max depth = 50 m.

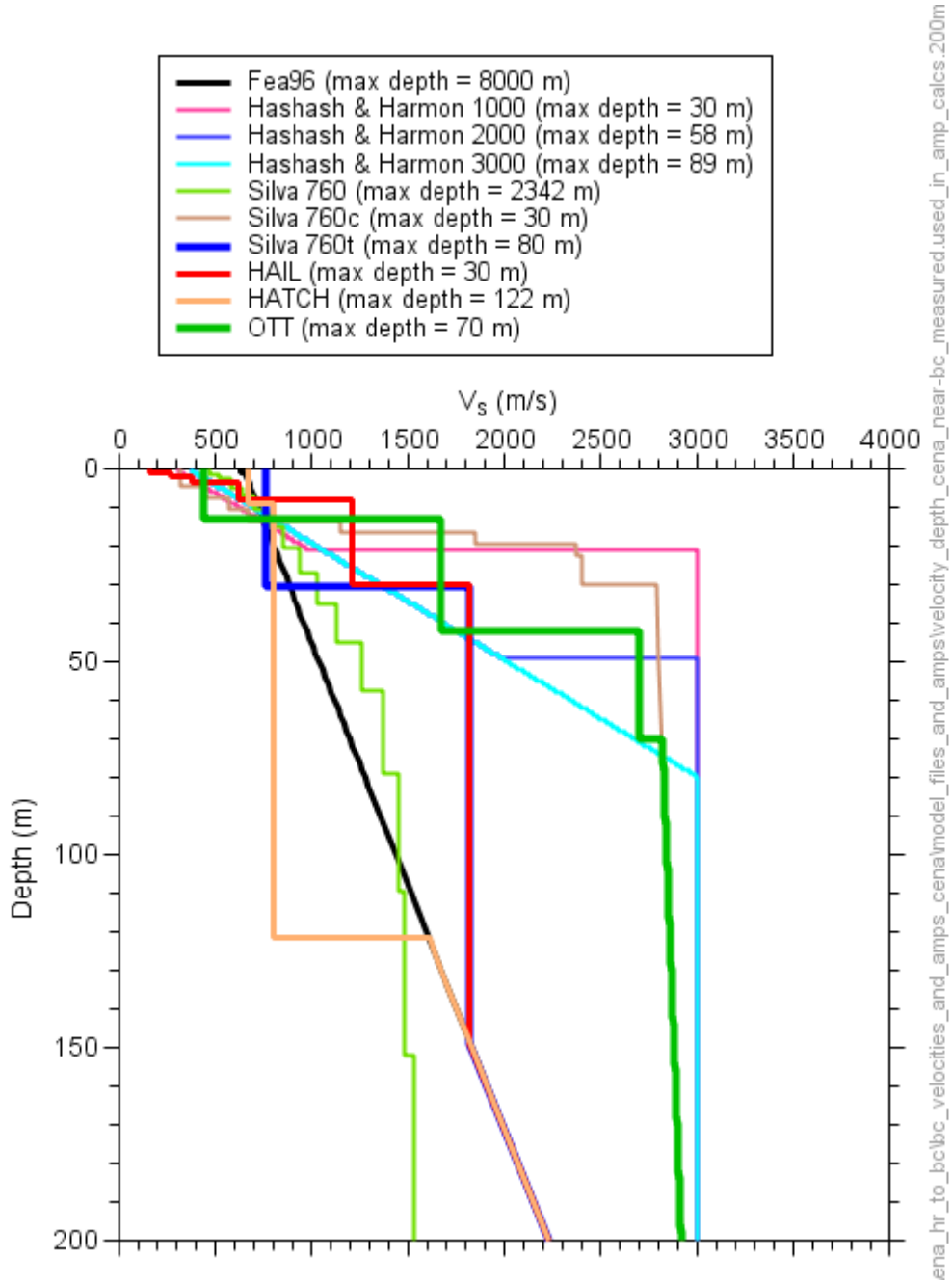

Figure 4. Combined profiles, max depth = 200 m.

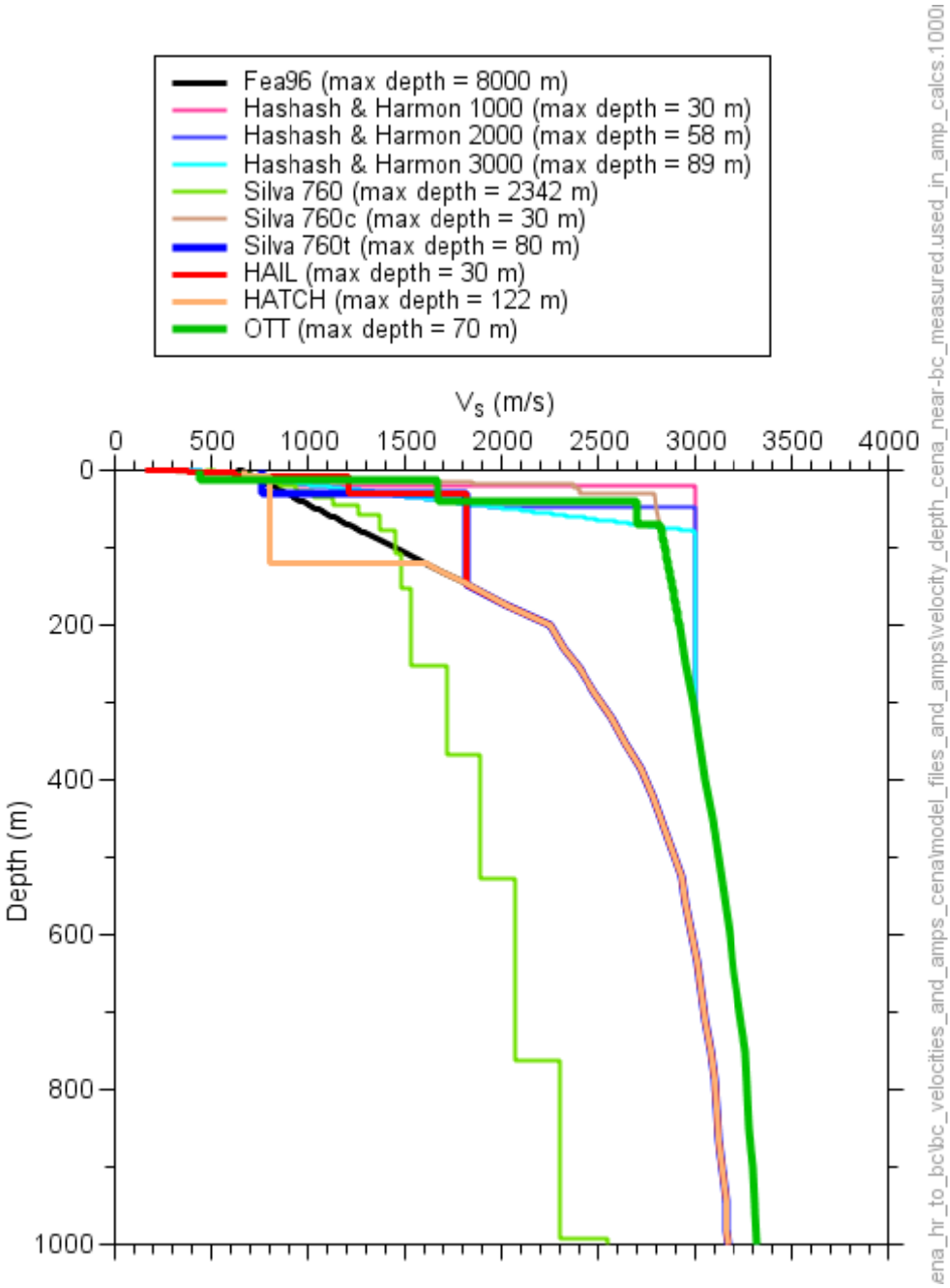

Figure 5. Combined profiles, max depth = 1000 m.

Amplifications for Sites with V_{S30} = 760 m/s:

I computed the square root impedance (SRI) amplifications for each of the profiles, using the method described in Boore (2013). The results are shown in Figure 6.

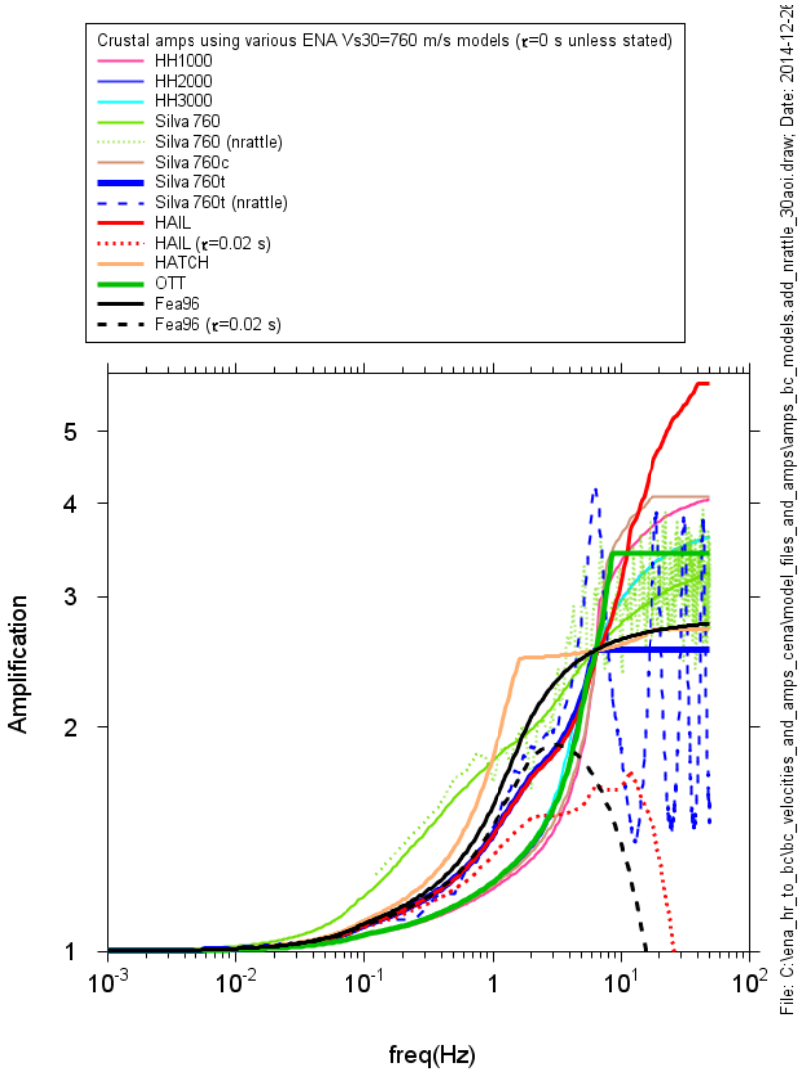

Figure 6. Amplifications from the square-root-impedance method (Boore, 2013) assuming an angle of incidence of 0 degrees; also shown are full-resonant amplifications (using the program *nrattle*) for two of the Silva profiles (one gradient like and one step like), assuming SH waves with a 30 degree angle of incidence. The effect of applying a kappa operator with k=0.02 s is also shown for two of the profiles. The Fea96 amplifications used a newer velocity-density relation than used to obtain the densities in Table A6 of Fea96, and therefore the amplifications shown in the figure are slightly different than those in Table A5 of Fea96.

Here are some comments on the amplifications shown in Figure 6: 1) the SRI amplifications all come together at a frequency corresponding to a quarter wavelength for 30 m, since each model has the same or almost the same Vs30; 2) the amplifications at lower frequencies are controlled by the deeper parts of the profiles, and since there are three deeper profiles, the amplifications for the ten shallow models merge into one of three amplification curves; 3) at higher frequencies the amplifications are controlled by the shallow parts of the models, which can have significant variations--but the attenuation operator will reduce the importance of these high frequencies when computing PSA at short periods; 4) the full resonant calculations are in reasonable agreement with both the gradient and step models (the underprediction of the resonant peaks for the step model is a well known limitation of the SRI method (see Boore, 2013)). My take on looking at the results is that the Frankel et al (Fea96) model is a reasonable compromise of the various models, and so the results in my notes *Adjusting PSA amplitudes to Vs30 3000.v01.pdf* from 19 November 2014 can be used. I have included the discussion of the simulations from those notes in a later section

Sites with V_{S30} = 3000 m / s

Velocity Profiles for Sites with V_{S30} = 3000 m/s:

The velocity profiles are based on the very hard rock profile of Boore and Joyner (1997). For $V_{S30} = 3000$ m/s , the top 300 m of the Boore and Joyner profile was replaced by a layer with a velocity of 3000 m/s (see Boore and Thompson, 2015). For $V_{S30} = 2000$ m/s , the top 30 m of the profile had a shear-wave velocity of 2000 m/s, and this was underlain by material with a linear gradient, joining the standard profile at a depth of 300 m. As described in Frankel et al. (1996), for $V_{S30} = 760$ m/s a linear gradient was added near the surface to give the proper value of V_{S30}.

Here is a plot of the velocities.

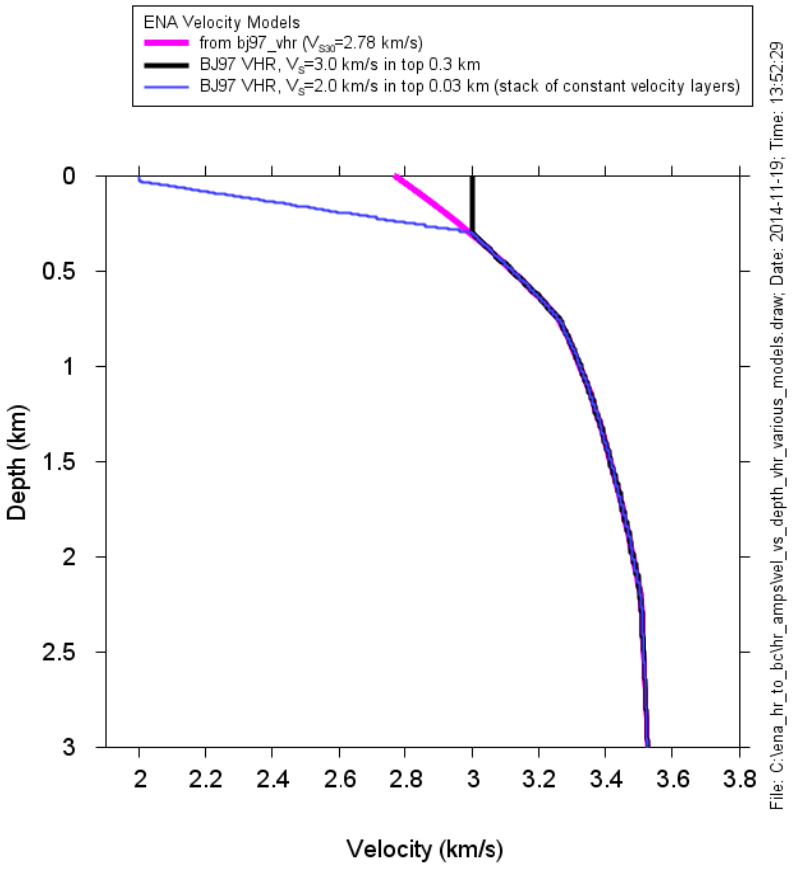

Figure 7.

Amplifications for sites with V_{S30} = 3000 m/s:

The amplifications were computed assuming a source density and velocity of 2.8 gm/cc and 3.7 km/s, assuming vertical angle of incidence and no attenuation (see Boore and Thompson, 2015, and my July, 2014 notes *Some notes on crustal amps_v01.pdf* for more detail). The amplifications are shown in Figure 8, along with those from an alternative ENA very hard rock model.

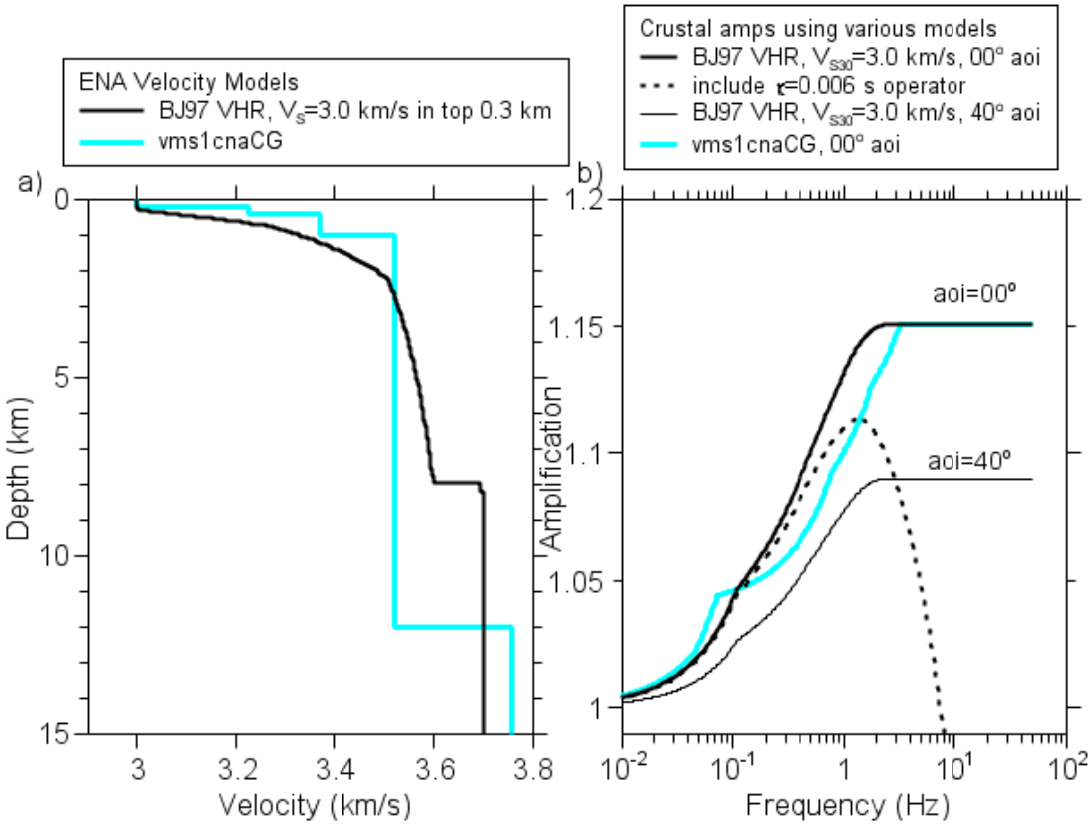

Figure 8. (from Boore and Thompson, 2015). a) Velocity models for a very hard rock (VHR) site in eastern North America (ENA); see Boore and Thompson (2015) for an explanation of the models. b) Amplifications for the two models; the amplification for the modified Boore and Joyner (1997) (BJ97) model is shown for two angles of incidence (*aoi*), without and with the κ attenuation operator for $aoi = 00^{\circ}$. The crustal amplifications for a $V_{S30} = 3000$ m/s site used in these notes are those for the modified BJ97 VHR model, assuming an angle of incidence (aoi) of 0 degrees.

Simulations and Ratios of PSA

I computed PSA and ratios for two very different path attenuation models: Atkinson (2004) (A04), with a steep decay of $1/R^{1.3}$ within the first 70 km, an increase going as $R^{0.2}$ from 70 to 140 km, followed by $1/R^{0.5}$ decay, and the Boatwright and Seekins (2011) (BS11) model, with $1/R^{1.0}$ within the first 50 km, followed by $1/R^{0.5}$. The *Q(f)* models differ for A04 and BS11.

The Boore and Thompson (2015) path durations were used. Other model parameters are contained in the SMSIM params files, available upon request. There is uncertainty about what value to use for κ for the $V_{S30} = 760$ m/s model. Frankel et al. (1996) used 0.01 s and 0.02 s was used by Silva et al. (1996) and Atkinson and Boore (2006). As will be seen in the ratio plots (and as discussed in draft manuscript by Boore and Campbell, titled *on_converting_vhr_to_bc_site_conditions_in_ena*, in preparation), the conversion factor from a BC condition to a very hard rock condition can be quite sensitive to the choice of κ for short period motions at close distances. For these notes I show ratios for κ equal to 0.01, 0.02, and 0.03 s. Here are the ratio plots:

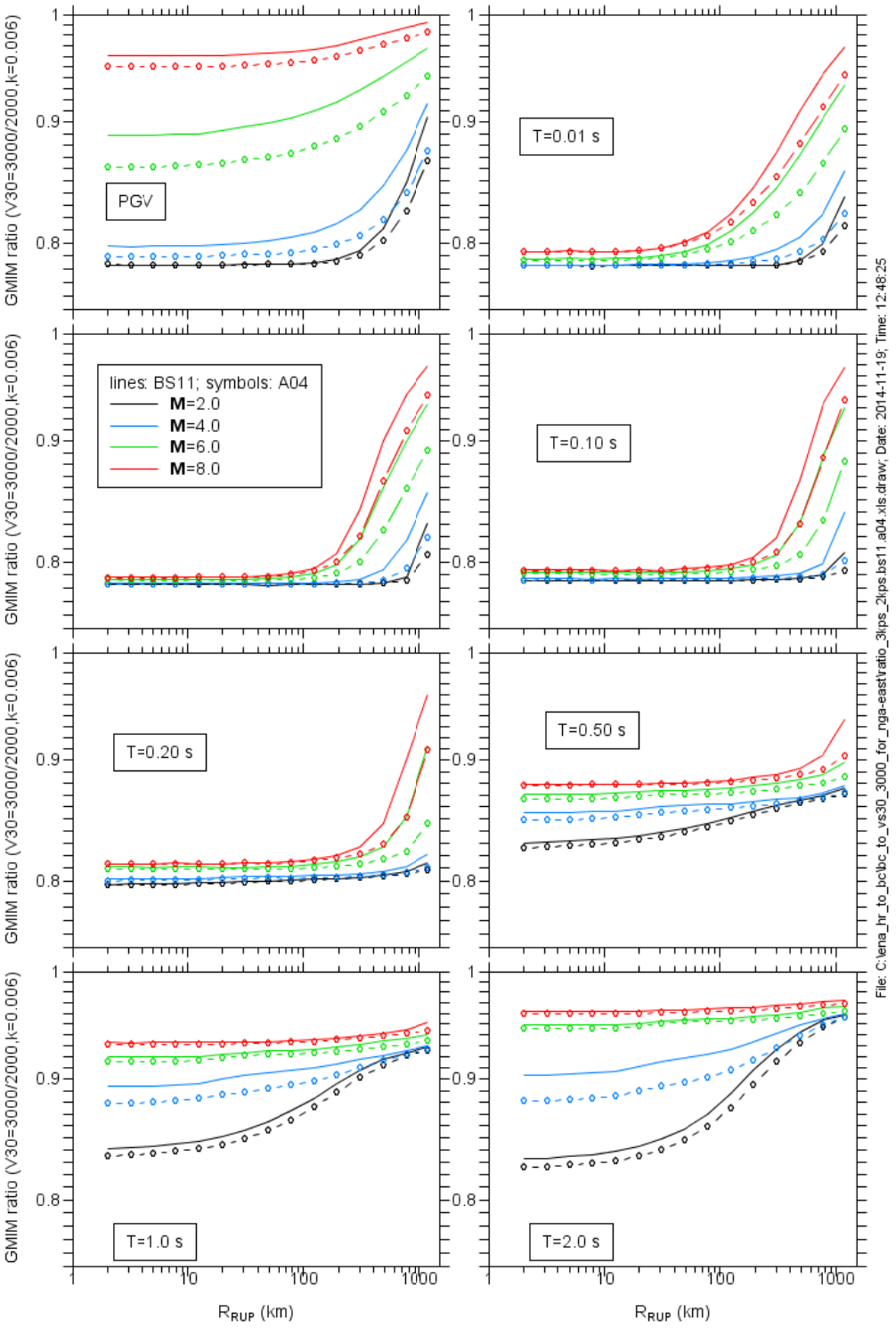

Figure 9. Ratios of PSA for $V_{S30} = 3000$ m/s and $V_{S30} = 2000$ m/s . k=0.006 s for both.

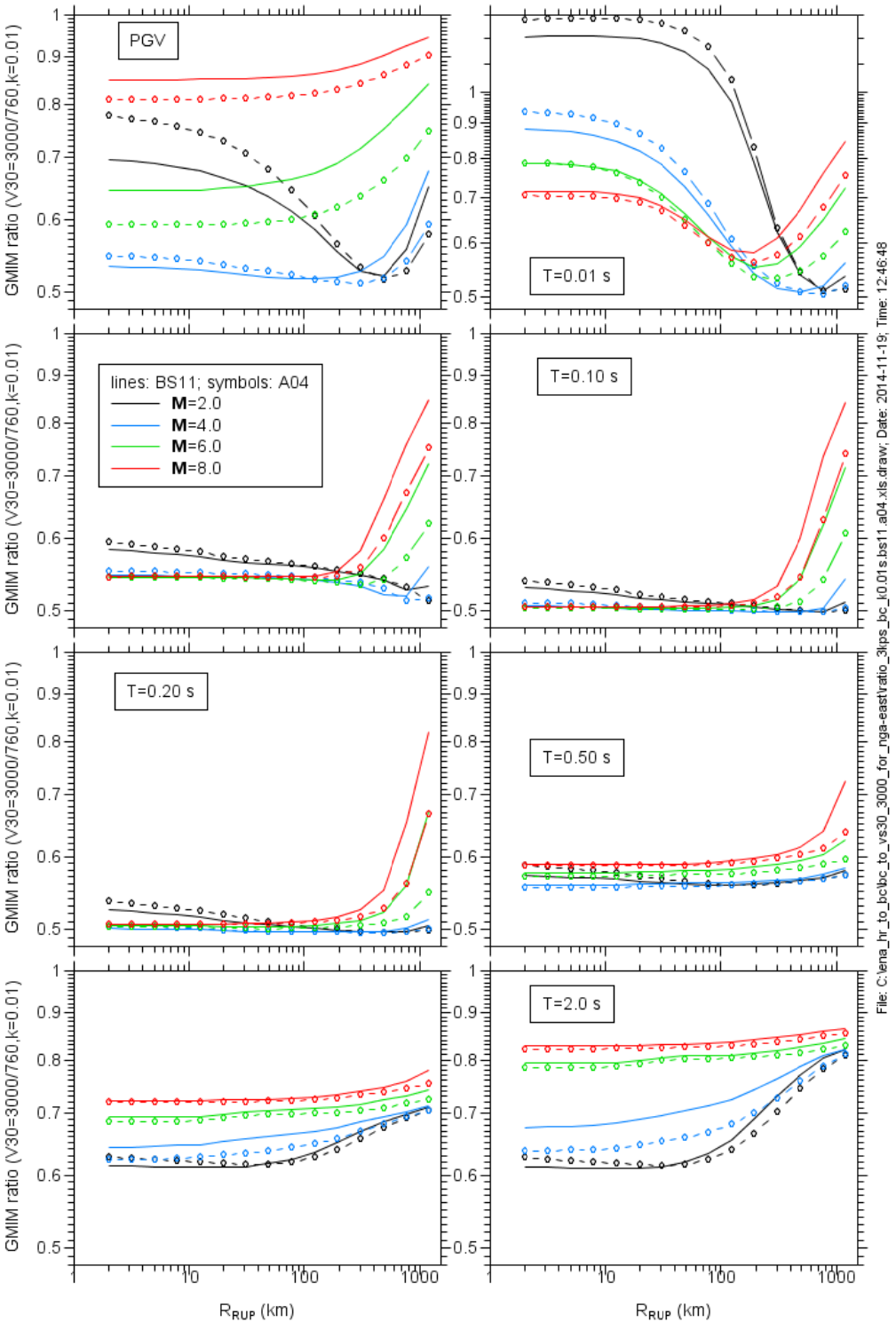

Figure 10. Ratios of PSA for V_{S30} = 3000 m/s , k=0.006 s, and V_{S30} = 760 m/s and k=0.01 s.

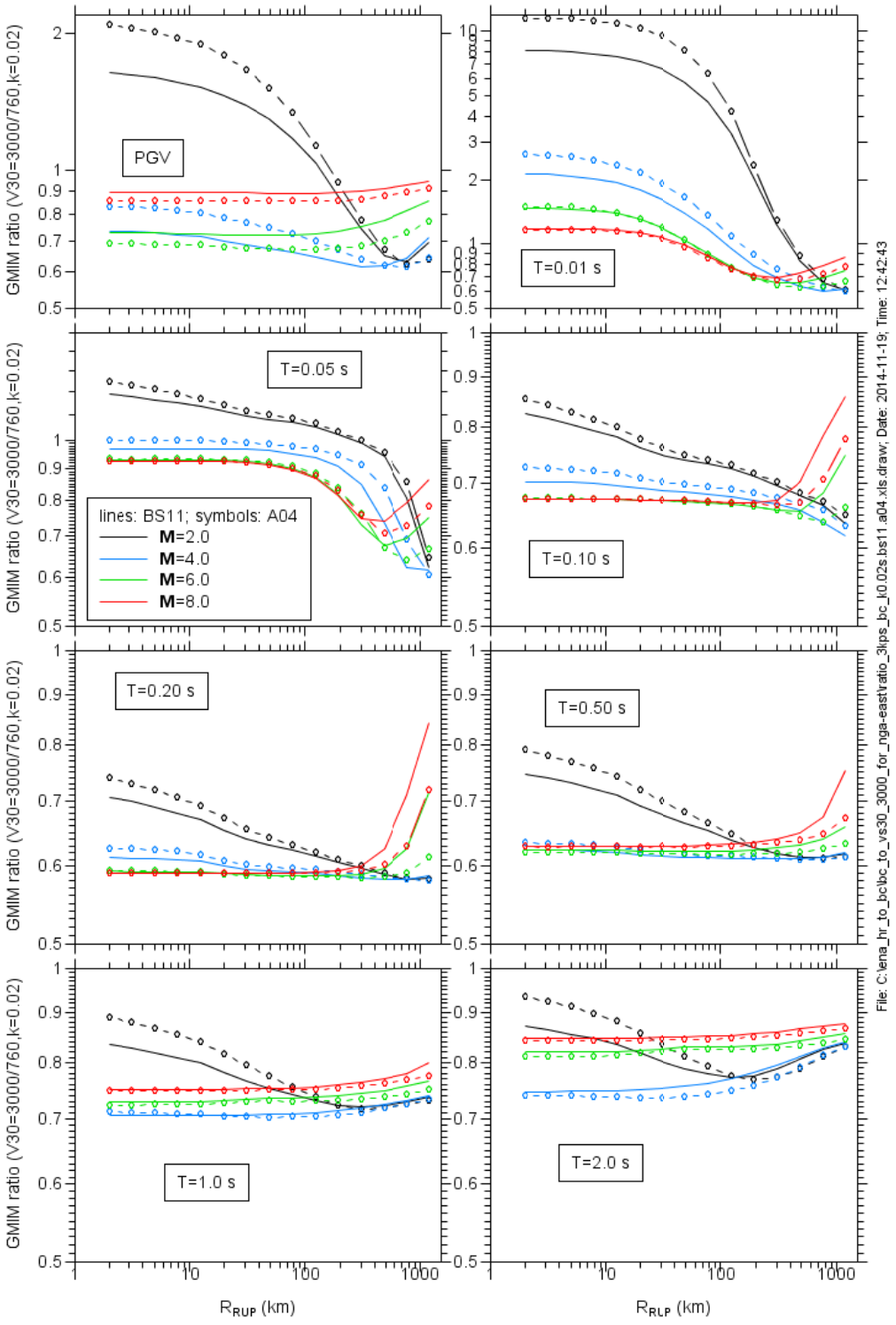

Figure 11. Ratios of PSA for V_{S30} = 3000 m/s , k=0.006 s, and V_{S30} = 760 m/s and k=0.02 s.

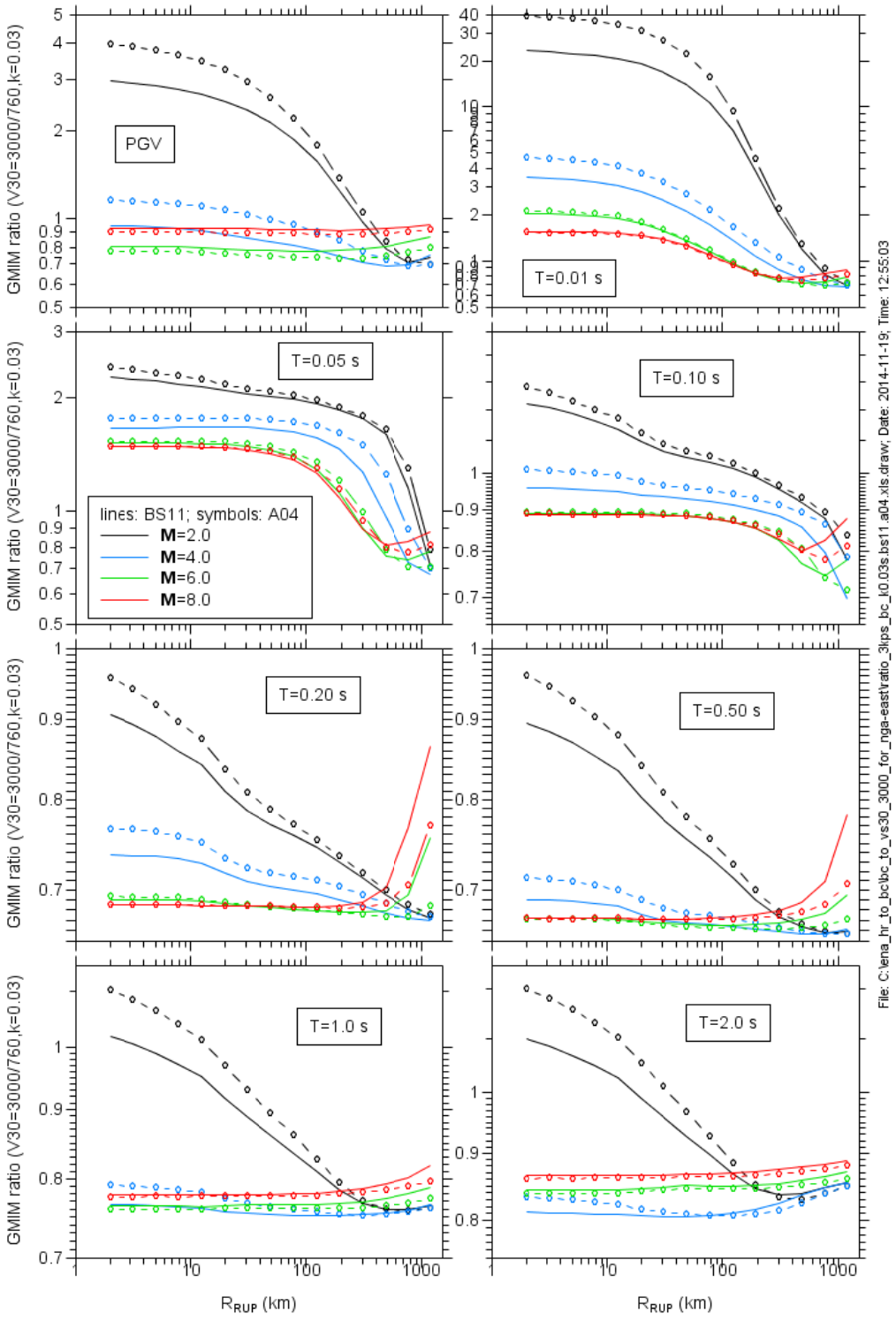

Figure 12. Ratios of PSA for V_{S30} = 3000 m/s , k=0.006 s, and V_{S30} = 760 m/s and k=0.03 s.

And now a direct comparison of the ratios for different kappas (different line types and widths, with the same color for each M).

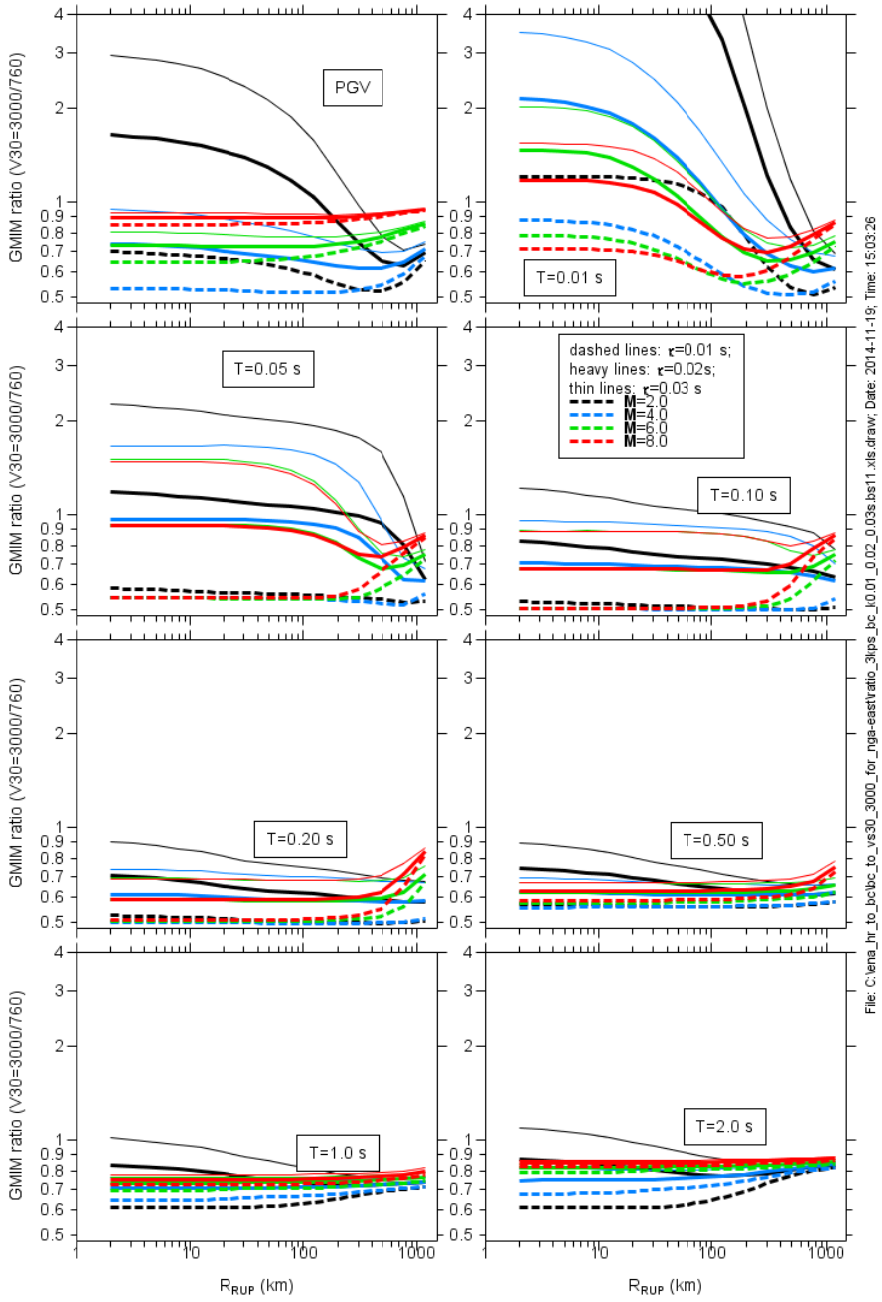

Figure 13. The BS11 attenuation model was used. To make the period-dependent sensitivity of the ratios clear, I used the same scale for the ordinate in all graphs (sacrificing the ratios for **M**=2 and T=0.01 s being onscale).

Here are a few observations (I welcome others to scrutinize the plots and reach their own conclusions, which could show my conclusions to be in the need of revision or addition):

1. The ratios for very small **M** are quite different than for those from larger **M**.

2. In general, the ratios are similar for the two path attenuation models.

3. Ignoring **M**=2, the ratios are somewhat insensitive to **M** and R, except for short periods and larger distances. This is good news, as it suggests that a simple period-dependent adjustment factor can be used for a wide range of **M** and R.

4. The ratios for short-period motions are very sensitive to the value of kappa. For example, the BC to 3000 m/s adjustment factors for **M**=6 for kappa=0.01 and 0.03 s differ by a factor of 1.8 for T=0.1 and a factor of 1.1 for T=1.0 for distances out to several hundred km.

I have not attempted to fit these ratios to equations with M, R, and k as predictor variables, but I have included the Excel files of ratios in case users want to use table lookup procedure to determine the Vs30=760-to-Vs30=3000 conversion factor to use in an application. These Excel files have these names:

ratio_3kps_2kps.a04.xls

ratio_3kps_2kps.bs11.xls

ratio_3kps_bc_k0.01s.a04.xls

ratio_3kps_bc_k0.01s.bs11.xls

ratio_3kps_bc_k0.02s.a04.xls

ratio_3kps_bc_k0.02s.bs11.xls

ratio_3kps_bc_k0.03s.a04.xls

ratio_3kps_bc_k0.03s.bs11.xls

The content of each file should be obvious from the file name ("kps"=km/s, "bc" is shorthand for Vs30=760 m/s).

References

Atkinson, G.M. (2004). Empirical attenuation of ground-motion spectral amplitudes in southeastern Canada and the northeastern United States, *Bull. Seism. Soc. Am.* **94,** 1079--1095.

Atkinson, G.M. and D.M. Boore (2006). Earthquake ground-motion prediction equations for eastern North America, *Bull. Seismol. Soc. Am.* **96**, 2181–2205. (also see the erratum published in Vol. 97, No. 3, p. 1032).

Beresnev, I.A. and G.M. Atkinson (1998). Shear-wave velocity survey of seismographic sites in eastern Canada calibration of empirical regression method of estimating site response, *Seismol. Res. Letters* **68**, 981–987.

Boatwright, J. and L. Seekins (2011). Regional spectral analysis of three moderate earthquakes in northeastern North America, *Bull. Seismol. Soc. Am.* **101**, 1769–1782.

Boore, D. M. (2005). SMSIM---Fortran Programs for Simulating Ground Motions from Earthquakes: Version 2.3---A Revision of OFR 96-80-A, U.S. Geological Survey Open-File Report, *U. S. Geological Survey Open-File Report* **00-509**, revised 15 August 2005, 55 pp. Available from the online publications link on http://www.daveboore.com .

Boore, D.M. (2013). The uses and limitations of the square-root impedance method for computing site amplification, *Bull. Seismol. Soc. Am.* **103**, 2356–2368.

Boore, D.M. and K.W. Campbell (20xx). On converting ground motions from very hard rock to NEHRP class BC site conditions in eastern North America, (in preparation).

Boore, D.M. and W.B. Joyner (1997). Site amplifications for generic rock sites, *Bull. Seismol. Soc. Am.* **87**, 327–341.

Boore, D.M. and E.M. Thompson (2015). Revisions to some parameters used in stochastic-method simulations of ground motion, *Bull. Seismol. Soc. Am.* **105**, (revised in response to the external reviews*). Available from* *http://www.daveboore.com/pubs_online.html*.

Frankel, A., C. Mueller, T. Barnhard, D. Perkins, E. Leyendecker, N. Dickman, S. Hanson, and M. Hopper (1996). National seismic hazard maps: documentation June 1996, *U. S. Geol. Surv. Open-File Rept.* **96-532**, 69 pp.

Hollenback (2014). PEER RVT Approach: Empirical FAS Model. Presented by Justin Hollenback at NGA-East SSHAC Workshop 3A, http://peer.berkeley.edu/ngaeast/wp-content/uploads/2014/09/Day2_AM_06_Hollenback_PEER_RVT_Approach_MinorRevisions.pdf (last accessed 19 November 2014).

Odum, J. K., W. J. Stephenson, and R. A. Williams (2010). Predicted and observed spectral response from collocated shallow, active and passive-source Vs data at five ANSS Sites, Illinois and Indiana, USA, *Seismol. Research Letters* **81**, 955–964.

Silva, W., R. Darragh, and N. Gregor (1999). Reassessment of site coefficients and near-fault factors for building code provisions, *U.S. Geol. Surv. Award 98-HQ-GR-1010*, final report.

Stewart, J.P., Y.M.A. Hashash, B. Kim, and J. Harmon (2012). Preliminary site corrections for NGA-East project, memo to Christine Goulet, dated November 3, 2012.